

Preparation of homopolymers from new azobenzene organic molecules with different terminal groups and study of their nonvolatile memory effects

Fei-Long Ye^{a,b}, Pei-Yang Gu^{a,b}, Feng Zhou^{a,b}, Hai-Feng Liu^{a,b}, Xiao-Ping Xu^{a,b}, Hua Li^{a,b}, Qing-Feng Xu^{a,b,*}, Jian-Mei Lu^{a,b,*}

^a Department of Polymer, College of Chemistry, Chemical Engineering and Materials Science, Soochow University, 199 Ren'ai Road, Suzhou 215123, China

^b Key Laboratory of Adsorption Technology in Petroleum and Chemical Industry for Wastewater Treatments, Soochow University, 199 Ren'ai Road, Suzhou 215123, China

ARTICLE INFO

Article history:

Received 5 January 2013

Received in revised form

12 April 2013

Accepted 17 April 2013

Available online 25 April 2013

Keywords:

Azo organic molecules

Homopolymers

Terminal group

ABSTRACT

Two new azo organic molecules Azo-OCH₃ and Azo-Br were synthesized by using electron-donating moiety methoxyphenyl and electron-accepting moiety bromophenyl as a terminal group respectively. Two monomers MAzo-OCH₃ and MAzo-Br based on them were also synthesized and corresponding homopolymers PAzo-OCH₃ and PAzo-Br were prepared by free radical polymerization. Azo-OCH₃ and Azo-Br were fabricated as films by vacuum evaporation while PAzo-OCH₃ and PAzo-Br were fabricated as films by simple spin-coating and all of them were then prepared as sandwich memory devices ITO/Azo-OCH₃/Al, ITO/Azo-Br/Al, ITO/PAzo-OCH₃/Al and ITO/PAzo-Br/Al respectively. According to the measurements, all devices exhibited stable binary WORM-type (write once and read many times) memory effects. However, ITO/Azo-OCH₃/Al and ITO/Azo-Br/Al exhibited different turn-on threshold voltages of about -2, -3.6 V respectively. It illustrated that to organic molecule anchoring electron-donor as a terminal group shows lower turn-on threshold voltage, which was related to low-power consumption. Moreover, the ITO/polymer/Al devices have successfully preserved the memory performance of devices based on corresponding organic molecules. Therefore, we successfully achieved the advantages of low-cost and low-power consumption by designing molecular structures and easy fabrication by polymerization.

Crown Copyright © 2013 Published by Elsevier Ltd. All rights reserved.

1. Introduction

In recent years, a great deal of effort has been devoted to developing fast, nonvolatile, and inexpensive techniques for data storage [1]. Among various memory devices, nonvolatile memory devices have been attracting considerable attention due to the low fabrication cost and 3D stacking to achieve low-cost but high-density memory [2–8]. Electroactive organic and polymeric materials are alternatives to traditional inorganic semiconductors that have to face the problem of scaling down in feature size [9–15]. Organic materials have the advantages of facile tailoring through organic synthesis and very low power consumption [16]. Thus, organic electrical memory devices appear highly attractive and have great potential application in data storage.

In comparison with organic molecule, polymer can be fabricated on the substrate by using a simple spin-coating technique or surface-initiated ATRP method [17,18]. The advantages of easy fabrication, high mechanical behavior and good scalability of polymers and polymer composites have attracted considerable attention in preparation of polymer-based devices and polymer composites-based devices [19–22], such as poly(9-(2-(4-vinyl(benzyloxy)ethyl)-9H-carbazole)) brushes and poly(N-vinylcarbazole)-graphene composites [18,23]. Among the reported polymers, flexible polymers pendent with functional groups have the obvious advantages for their rich diversities of structures, various polymerization methods. For example, the Kang group reported two poly(N-vinylcarbazole) copolymers with pendent azobenzene chromophores PVK-AZO-NO₂ and PVK-AZO-2CN. The terminal electron acceptor moieties of the two copolymers are strong electron-withdrawing groups, -NO₂ and -CN respectively. Both of them exhibit write-once-read-many-times (WORM) type memory effects owing to the deep electron traps caused by the strong electron acceptors [24]. In addition, it's worthy of mention that quite a few organic molecules and

* Corresponding authors. Department of Polymer, College of Chemistry, Chemical Engineering and Materials Science, Soochow University, 199 Ren'ai Road, Suzhou 215123, China. Tel./fax: +86 512 6588 0367.

E-mail addresses: xuqingfeng@suda.edu.cn (Q.-F. Xu), lujm@suda.edu.cn (J.-M. Lu).

polymers have been considered as active materials for memory devices [25,26]. However, few reports have focused on the differences and connections between organic molecules-based memory devices and corresponding polymers-based memory devices.

In this paper, we synthesized two new azo organic molecules Azo-OCH₃ and Azo-Br firstly. Azo-OCH₃ and Azo-Br have longer conjugation length than most of other reported organic molecules by introducing azobenzene and acrylonitrile groups. The long conjugation length of Azo-OCH₃ and Azo-Br was designed for the stable memory property. The WORM memory effects can be predicted due to the strong electron-withdrawing ability of cyano group. Meanwhile, we introduced donating and accepting electronic moieties to the end of azo organic molecules respectively for studying the relationship between electrical memory behavior and terminal electron moieties. In addition, the corresponding homopolymers (PAzo-OCH₃ and PAzo-Br) were prepared for easier device fabrication. Azo-OCH₃, Azo-Br, PAzo-OCH₃ and PAzo-Br all exhibit excellent WORM memory behavior. In polymer-based devices, the memory effects were well-preserved. Interestingly, both Azo-OCH₃ and PAzo-OCH₃ based devices have an advantage of possessing low turn-on threshold voltage due to the effective electron-donor terminal group.

2. Experimental section

2.1. Materials

4-Aminobenzaldehyde Polymer, 3,4-dimethoxyphenylacetonitrile, 4-bromobenzyl cyanide, sodium hydride, AIBN were all purchased from Shanghai Chemical Reagent Co. Ltd. as analytical reagents and used as received. N-Ethyl-N-(2-hydroxyethyl)aniline was purchased from Tokyo Kasei Kogyo Co. Ltd. and used as received. Methacryloyl chloride was obtained from Haimen Best Fine Chemical Industry Co. Ltd. and used after distillation. Sodium acetate anhydrous, sodium

nitrite and other solvents were used as received without any further purification.

2.2. Preparation of Azo-OCH₃, Azo-Br, PAzo-OCH₃ and PAzo-Br

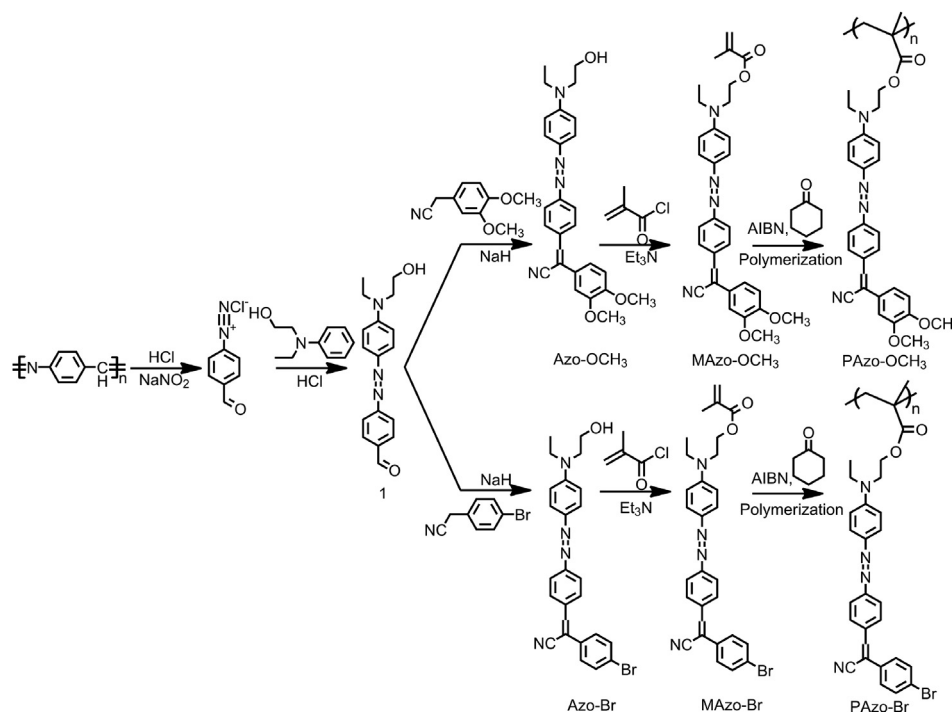
Synthesis scheme and molecular structures of Azo-OCH₃, Azo-Br, PAzo-OCH₃ and PAzo-Br are shown in Scheme 1.

2.2.1. Synthesis of 4-((4-(ethyl(2-hydroxyethyl)amino)phenyl) diazenyl)benzaldehyde (compound 1)

A solution of sodium nitrite (4.35 g, 0.063 mol) in water (24 mL) was added dropwise to the mixture of 4-aminobenzaldehyde polymer (6.03 g, 0.06 mol), water (32 mL) and concentrated hydrochloric (20 mL) at 0–5 °C. The mixture was stirred at 0–5 °C for 30 min. The mixture of N-ethyl-N-(2-hydroxyethyl)aniline (10.89 g, 0.066 mol), concentrated hydrochloric (10 mL) and water (30 mL) was added slowly to the diazonium salt solution at 0–5 °C. After 1 h, sodium acetate anhydrous (18 g, 0.22 mol) was added to the resultant mixture. The resultant mixture was stirred at 0–5 °C for 24 h. The solution was filtered, and the obtained crude product was recrystallized from ethanol to give the brown powder compound 1 (yield 68%). ¹H NMR (300 MHz, DMSO-*d*₆) δ (ppm): 10.05 (s, 1H), 8.04 (d, *J* = 8.4 Hz, 2H), 7.91 (d, *J* = 8.3 Hz, 2H), 7.81 (d, *J* = 9.1 Hz, 2H), 6.86 (d, *J* = 9.2 Hz, 2H), 4.85 (t, *J* = 5.2 Hz, 1H), 3.67–3.42 (m, 6H), 1.15 (t, *J* = 6.9 Hz, 3H). Anal. calcd. for C₁₇H₁₉N₃O₂: C, 68.61; H, 6.39; N, 14.12. Found: C, 68.52; H, 6.52; N, 13.98.

2.2.2. Synthesis of 2-(3,4-dimethoxyphenyl)-3-(4-(4-(ethyl(2-hydroxyethyl)amino)phenyl diazen-yl)phenyl)acrylonitrile (Azo-OCH₃)

A mixture of compound 1 (7.65 g, 0.0258 mol), 3,4-dimethoxyphenylacetonitrile (4.64 g, 0.0262 mol) and sodium hydride (312 mg, 0.013 mol) and anhydrous ethanol (100 mL) was refluxed at 84 °C for 12 h under N₂ protection. The reaction mixture



Scheme 1. Synthesis scheme and molecular structures of Azo-OCH₃, Azo-Br, PAzo-OCH₃ and PAzo-Br.

was cooled down and poured into 300 mL deionized water. The crude product was filtered off and recrystallized from ethanol to give the red powder Azo-OCH₃ (yield 82%). ¹H NMR (300 MHz, DMSO-*d*₆) δ (ppm): 8.11–8.00 (m, 3H), 7.88 (d, *J* = 8.6 Hz, 2H), 7.80 (d, *J* = 9.0 Hz, 2H), 7.38 (s, 1H), 7.30 (d, *J* = 8.4 Hz, 1H), 7.10 (d, *J* = 8.6 Hz, 1H), 6.86 (d, *J* = 9.2 Hz, 2H), 4.85 (s, 1H), 3.87 (s, 3H), 3.82 (s, 3H), 3.61 (s, 2H), 3.55–3.46 (m, 4H), 1.15 (t, *J* = 6.9 Hz, 3H). Anal. calcd. for C₂₇H₂₈N₄O₃: C, 70.97; H, 6.13; N, 12.27. Found: C, 70.89; H, 6.15; N, 12.32.

2.2.3. Synthesis of 2-(4-bromophenyl)-3-(4-(4-(ethyl(2-hydroxyethyl)amino)phenyl diazenyl) phenyl)acrylonitrile (Azo-Br)

A mixture of compound 1 (7.65 g, 0.0258 mol), 4-bromobenzyl cyanide (5.08 g, 0.0262 mol) and sodium hydride (312 mg, 0.013 mol) and anhydrous ethanol (100 mL) was refluxed at 84 °C for 12 h under N₂ protection. The reaction mixture was cooled down, then evaporated the excess solvent. The crude product was purified by column chromatography (petroleum ether:ethyl acetate 1:1, *v/v*) to give the red powder Azo-Br (yield 64%). ¹H NMR (300 MHz, DMSO-*d*₆) δ (ppm): 8.16 (s, 1H), 8.10 (d, *J* = 8.6 Hz, 2H), 7.89 (d, *J* = 8.5 Hz, 2H), 7.85–7.68 (m, 6H), 6.86 (d, *J* = 9.2 Hz, 2H), 4.84 (s, 1H), 3.67–3.41 (m, 6H), 1.15 (t, *J* = 6.9 Hz, 3H). Anal. calcd. for C₂₅H₂₃BrN₄O: C, 63.11; H, 4.84; N, 11.78. Found: C, 63.09; H, 5.00; N, 11.43.

2.2.4. Synthesis of 2-((4-(4-(2-cyano-2-(3,4-dimethoxyphenyl) vinyl)phenyl diazenyl)phenyl)ethyl-amino)ethyl methacrylate (MAzo-OCH₃)

Azo-OCH₃ (0.0025 mol) and Et₃N (2.0 g, 0.0075 mol) were added into freshly distilled tetrahydrofuran (THF; 40 mL) and stirred vigorously at 0 °C under nitrogen atmosphere. The acryloyl chloride (0.005 mol) solution in THF (20 mL) was added dropwise to the mixture. After 1 h, the ice-water bath was removed and the reaction was allowed to continue for 24 h at room temperature. The solution was filtered and poured into a large amount of water. The precipitated product was washed by column chromatography (petroleum ether:ethyl acetate 1:1, *v/v*) to give the red powder MAzo-OCH₃ (yield 72%). ¹H NMR (300 MHz, DMSO-*d*₆) δ (ppm): 8.13–8.00 (m, 3H), 7.90 (d, *J* = 8.4 Hz, 2H), 7.81 (d, *J* = 9.0 Hz, 2H), 7.39 (s, 1H), 7.31 (d, *J* = 8.4 Hz, 1H), 7.10 (d, *J* = 8.5 Hz, 1H), 6.93 (d, *J* = 9.1 Hz, 2H), 6.02 (s, 1H), 5.69 (s, 1H), 4.32 (s, 2H), 3.88 (s, 3H), 3.82 (s, 3H), 3.77 (s, 2H), 3.54 (d, *J* = 6.9 Hz, 2H), 1.86 (s, 3H), 1.16 (t, *J* = 6.8 Hz, 3H). Anal. calcd. for C₃₁H₃₂N₄O₄: C, 70.91; H, 6.10; N, 10.67. Found: C, 70.85; H, 6.15; N, 10.56.

2.2.5. Synthesis of 2-((4-(4-(2-cyano-2-(4-bromophenyl) vinyl) phenyl diazenyl)phenyl)ethylamino)ethyl methacrylate (MAzo-Br)

The synthesis method of MAzo-Br is similar with MAzo-OCH₃. (Yield 68%). ¹H NMR (300 MHz, DMSO-*d*₆) δ (ppm): 8.17 (s, 1H), 8.11 (d, *J* = 8.5 Hz, 2H), 7.90 (d, *J* = 8.5 Hz, 2H), 7.86–7.68 (m, 6H), 6.93 (d, *J* = 9.1 Hz, 2H), 6.02 (s, 1H), 5.68 (s, 1H), 4.32 (s, 2H), 3.77 (s, 2H), 3.54 (d, *J* = 6.8 Hz, 2H), 1.86 (s, 3H), 1.16 (t, *J* = 6.8 Hz, 3H). Anal. calcd. for C₂₉H₂₇BrN₄O₂: C, 64.03; H, 4.97; N, 10.30. Found: C, 63.94; H, 5.05; N, 10.24.

2.2.6. Synthesis of poly 2-((4-(4-(2-cyano-2-(3,4-dimethoxyphenyl) vinyl)phenyl diazenyl)phenyl) ethylamino)ethyl methacrylate (PAzo-OCH₃) and poly 2-((4-(4-(2-cyano-2-(4-bromophenyl) vinyl)phenyl diazenyl)phenyl)ethylamino)ethyl methacrylate (PAzo-Br)

Monomer (1 mmol) was polymerized via free-radical polymerization in the presence of AIBN (0.1 mmol) initiator. The polymerization was carried out at 60 °C in cyclohexanone (5 mL) and under a nitrogen atmosphere for 48 h. The crude polymers were precipitated in 200 mL of methanol under vigorous stirring. The crude

polymers were purified by Soxhlet extractor with ethanol to remove of excess monomers and get the azo polymers PAzo-OCH₃ (Fig. S1, Supplementary Material) and PAzo-Br (Fig. S2, Supplementary Material) (yield 78%).

2.3. Characterization

¹H NMR spectra were obtained on an Inova 300 MHz FT-NMR spectrometer at ambient temperature. Molecular weights (*M_n*) and polydispersity (*M_w/M_n*) were measured by gel permeation chromatography (GPC) utilizing a Waters 515 pump and a differential refractometer. DMF was used as a mobile phase at a flow rate of 1.0 mL/min. Thermogravimetric analysis (TGA) was conducted on a TA Instruments Dynamic TGA 2950 at a heating rate of 10 °C/min and under an N₂ flow rate of 50 mL/min. Ultraviolet–visible (UV–vis) absorption spectra were recorded on a Perkin–Elmer Lambda spectrophotometer. Electrochemical properties of azo organic molecules (Azo-OCH₃ and Azo-Br) were investigated by using conducting cyclic voltammetry measurements in DMF solution (10⁻³ mol/L). A 0.1 M solution of tetrabutylammonium hexafluorophosphate in anhydrous DMF was used as an electrolyte. Cyclic voltammetry was performed at room temperature using a platinum wire electrode as the working electrode, a platinum gauze electrode as a counter electrode and an Ag/AgCl electrode as a reference electrode at a sweep rate of 1 mV s⁻¹. The electrochemical properties of azo polymers (PAzo-OCH₃ and PAzo-Br) were investigated by using conducting cyclic voltammetry measurements in acetonitrile solution. A 0.1 M solution of tetrabutylammonium hexafluorophosphate in anhydrous acetonitrile was used as an electrolyte. Cyclic voltammetry was performed at room temperature using an ITO electrode as the working electrode, a platinum gauze electrode as a counter electrode and an Ag/AgCl electrode as a reference electrode at a sweep rate of 1 mV s⁻¹ (CHI 604C electrochemical analyzer). Atomic force microscopy (AFM) measurements were obtained with a NanoScope 3D Controller atomic force microscope (Digital Instruments) operated in the tapping mode at room temperature.

2.4. Fabrication of the organic molecule memory device

The indium tin oxide (ITO) glass was pre-cleaned with water, acetone, and isopropanol each for 15 min. The organic thin films were vacuum evaporated in a vacuum deposition apparatus, take about 20 mg of organic compounds on the evaporator furnace and drawn about the degree of vacuum to 3 × 10⁻⁴ Pa. The organic compounds in the evaporator furnace were slowly sublimated to the ITO glass surface. The organic molecule films were annealed in a vacuum chamber at 10⁻⁵ torr and 80 °C for 12 h. The organic molecule film thickness was around 100 nm (Fig. S3, Supplementary Material).

2.5. Fabrication of the polymer memory device

The azo polymer solution was prepared in 1,2-dichloroethane (10 mg/mL) and filtered through microfilters with a pinhole size of 0.22 μm. Then, the filtered solution was spin-coated onto the pre-cleaned ITO glass at a speed rate of 2000 rpm for 40 s and the solvent was removed in a vacuum chamber at 10⁻⁵ torr and 60 °C for 12 h. The polymer film thickness was around 100 nm (Fig. S3, Supplementary Material). Al top electrodes were thermally evaporated and deposited onto the polymer surface at about 10⁻⁷ torr through a shadow mask. The current–voltage (*I*–*V*) characteristics were performed using an HP 4145B semiconductor parametric analyzer. All electrical measurements of the devices were characterized under ambient conditions.

3. Results and discussion

3.1. Polymer characterization

Synthesis scheme and molecular structures of PAzo-OCH₃ and PAzo-Br are shown in Scheme 1. GPC showed that the number-average molecular weights of PAzo-OCH₃ and PAzo-Br were about 8030 with a polydispersity index (PDI) of 1.59 and 8120 with PDI of 1.64 respectively.

3.2. Thermal stabilities

The thermal properties of the azo organic molecules and the azo polymers were evaluated by TGA under nitrogen atmosphere (Fig. S4, Supplementary Material). The 5% weight-lost temperature ($T_{d5\%}$) of Azo-OCH₃, Azo-Br, PAzo-OCH₃ and PAzo-Br was found to be 274 °C, 302 °C, 295 °C and 292 °C respectively. The good thermal stability of the azo organic molecules and the azo polymers is essential for their applications as active materials in electronic devices [27]. Glass transition temperatures of azo polymers were evaluated by DSC under nitrogen atmosphere. The glass transition temperatures (T_g) of PAzo-OCH₃ and PAzo-Br were found to be 103 °C and 108 °C respectively.

3.3. Optical properties

The absorption spectra of Azo-OCH₃, Azo-Br, PAzo-OCH₃ and PAzo-Br in THF solution and thin film state are shown in Fig. 1 and summarized in Table 1 respectively. All of them exhibit two major absorption peaks according to Fig. 1. The absorption peak of azo organic molecules at the shorter wavelength (around 350 nm) is attributed to the $\pi-\pi^*$ electronic transition of the aromatic ring, while the peak at the longer wavelength (around 480 nm) is due to the coupling between the $n-\pi^*$ and $\pi-\pi^*$ transitions of the azo-benzene chromophore and acrylonitrile chromophore [24,28]. Absorption peaks are red-shifted when electron withdrawing ability of the terminal substituent increased, which might be attributed to the increased electron transition ability and the increased electron delocalization. Compared to those of azo organic molecules, the absorption bands of azo polymers are evidently blue-shifted (459 nm for PAzo-OCH₃ and 463 nm for PAzo-Br), which is ascribed to the formation of flexible main chain. In addition, compared with the absorption spectra in solution, both the $\pi-\pi^*$ transition and the CT transition absorption peaks are bathochromic-shifted and broadened in film state, ascribed to the formation of molecular aggregation [29].

3.4. Electrochemical properties

The electrochemical properties of azo organic molecules (Azo-OCH₃ and Azo-Br) and azo polymers (PAzo-OCH₃ and PAzo-Br) were investigated by using conducting cyclic voltammetry measurements, as shown in Fig. 2 and summarized in Table 1.

The highest occupied molecular orbital (HOMO) and lowest unoccupied molecular orbital (LUMO) energy levels can be calculated from the UV visible absorption spectra and the cyclic voltammetry (CV) results by the following equations [30]:

$$E_{\text{HOMO}} = -[E_{\text{Ox}} + 4.8 - E_{\text{Foc}}]$$

$$E_{\text{LUMO}} = E_{\text{HOMO}} + E_g$$

where E_{ox} is the onset oxidation potential, E_{Foc} is the external standard potential of the ferrocene/ferrocenium ion couple and E_g is the band gap determined from the UV–visible absorption. The optical band gaps of Azo-OCH₃, Azo-Br, PAzo-OCH₃ and PAzo-Br estimated from the absorption edges are 2.25, 2.21, 2.19 and 2.18 eV, respectively. The external ferrocene/ferrocenium (Fc/Fc⁺) redox standard potential (E_{Foc1}) was measured to be 0.55 eV in DMF. The onset oxidation (E_{ox}) estimated from the cyclic voltammetry (CV) curve for the thin films of Azo-OCH₃ and Azo-Br is 1.03 and 1.20 eV respectively. The E_{Foc2} is 0.43 eV from the CV measurement without any polymer film coated on ITO glass. The onset oxidation (E_{ox}) estimated from the cyclic voltammetry (CV) curve for thin films of PAzo-OCH₃ and PAzo-Br is 0.92 and 1.18 eV respectively. The highest occupied molecular orbital (HOMO) energy levels of Azo-OCH₃, Azo-Br, PAzo-OCH₃ and PAzo-Br are determined to be -5.28, -5.45, -5.29 and -5.55 eV, respectively. The lowest unoccupied molecular orbital (LUMO) energy levels of Azo-OCH₃, Azo-Br, PAzo-OCH₃ and PAzo-Br are determined to be -3.03, -3.24, -3.10 and -3.37 eV, respectively. Optoelectronic properties and calculated energy levels of all compounds are summarized in Table 1.

The energy barrier to hole injection from the ITO electrode to the HOMO of Azo-OCH₃, Azo-Br, PAzo-OCH₃ and PAzo-Br was estimated to be 0.48, 0.65, 0.49 and 0.75 eV, respectively. The energy barrier to electron injection from the Al electrode to the LUMO of Azo-OCH₃, Azo-Br, PAzo-OCH₃ and PAzo-Br was estimated to be 1.25, 1.04, 1.18 and 0.91 eV, respectively.

It's clearly that hole injection from ITO into the HOMO is easier than electron injection from Al into the LUMO. Hence, Azo-OCH₃, Azo-Br, PAzo-OCH₃ and PAzo-Br are all p-type materials and the conduction process in these devices is dominated by hole injection as well [31]. The results indicate that ITO/Azo-OCH₃/Al device and

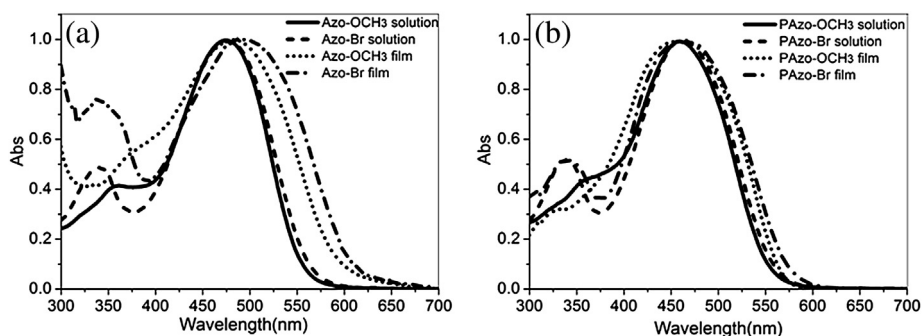


Fig. 1. (a) UV–vis absorption spectra of Azo-OCH₃, Azo-Br in dilute THF solution and solid thin film on ITO substrate; (b) UV–vis absorption spectra of PAzo-OCH₃, PAzo-Br in dilute THF solution and solid thin film on ITO substrate.

Table 1
Optoelectronic properties and calculated energy levels of all compounds.

Compound	UV–vis, λ_{\max} (nm)		E_g (eV)		E (V)	HOMO (eV)		LUMO (eV)	
	Soln ^a	Film	Calc	Exp ^b	E_{ox} (onset)	Calc	Exp ^c	Calc	Exp
Azo-OCH ₃	474	484	2.92	2.25	1.03	–5.21	–5.28	–2.29	–3.03
Azo-Br	477	487	2.86	2.21	1.20	–5.33	–5.45	–2.47	–3.24
PAzo-OCH ₃	459	461	2.91	2.19	0.92	–5.22	–5.29	–2.31	–3.10
PAzo-Br	463	467	2.86	2.18	1.18	–5.34	–5.55	–2.48	–3.37

^a In THF dilute solution.

^b Estimated from the absorption edge of the film.

^c The HOMO energy levels were calculated from cyclic voltammetry and were referenced to ferrocene (4.8 eV).

ITO/PAzo-OCH₃/Al device have lower hole-injection barrier than ITO/Azo-Br/Al device and ITO/PAzo-Br/Al device.

3.5. Electrical switching behavior of ITO/organic molecule/Al memory devices and ITO/polymer/Al memory devices

The memory behavior of Azo-OCH₃ and Azo-Br was tested by the I – V characteristics of ITO/organic molecule/Al devices. Organic molecule memory devices store data based on the high- and low-conductivity response to the external applied voltages. Fig. 3 shows typical I – V characteristics of the memory devices fabricated with azo organic molecules (Azo-OCH₃ and Azo-Br).

For ITO/Azo-OCH₃/Al, the first sweep was from 0 to –6 V. In the sweep from 0 to –2 V, the device was in the low-conductivity (OFF) state. When the sweep voltage switching threshold voltage of –2 V was reached, the current density increased abruptly from 10^{-6} to 10^{-2} A, indicating the device transition from the initial OFF state to the high-conductivity (ON) state. This electrical transition can serve as the “writing” process in a memory device. The device remained in the ON state during the subsequent negative sweep (0 to –6 V) and positive sweep (0–6 V), and it did not return to the OFF state even after turning off the power or upon applying a reverse sweep. The nonvolatile of the ON state suggests that ITO/Azo-OCH₃/Al device exhibits WORM type memory. ITO/Azo-Br/Al device was measured under the same conditions and a similar phenomenon was observed when voltage was added. More interestingly, the turn-on threshold voltages of two devices are different about –2 V for Azo-OCH₃, –3.6 V for Azo-Br and ON/OFF ratio is about 10^3 – 10^4 (Azo-OCH₃), 10^5 (Azo-Br) respectively. The results may indicate that ITO/Azo-OCH₃/Al device could provide a lower turn-on voltage, which means a low-energy cost write process.

Because the conduction process in these devices is dominated by hole injection, ITO/Azo-OCH₃/Al device has lower hole-injection barrier, thus holes can very efficiently be injected into the HOMO orbital of Azo-OCH₃. Different HOMO energy levels affect the turn-on threshold, while the higher HOMO level of Azo-OCH₃ resulted into a lower turn-on voltage [32]. Therefore, we can decrease the

turn-on voltage of memory devices by adopting the electron donating terminal moieties.

The memory behavior of PAzo-OCH₃ and PAzo-Br was tested by the I – V characteristics of ITO/polymer/Al devices. Fig. 4 shows typical I – V characteristics of the memory devices fabricated with azo polymers (PAzo-OCH₃ and PAzo-Br). The ITO/polymer/Al devices were measured under the same conditions with ITO/organic molecule/Al devices. ITO/PAzo-OCH₃/Al device has turn-on threshold voltage of about –2.4 V and ON/OFF ratio of about 10^3 – 10^4 while ITO/PAzo-Br/Al device has turn-on threshold voltage of about –4 V and ON/OFF ratio of about 10^5 .

The I – V curves suggested that the ITO/polymer/Al devices could provide similar turn-on voltage and ON/OFF ratio with corresponding ITO/organic molecule/Al devices. Hence, the ITO/polymer/Al devices maintained the data storage performance of the ITO/organic molecule/Al devices. Since organic molecule devices require more elaborate and expensive processing such as vacuum evaporation and deposition, it needs high fabrication cost to fabricate organic molecules into memory devices. Compared to organic molecule-based devices (ITO/Azo-OCH₃/Al and ITO/Azo-Br/Al), polymer-based devices (ITO/PAzo-OCH₃/Al and ITO/PAzo-Br/Al) not only have the advantages of easy fabrication, high mechanical flexibility and good scalability, but also their properties can easily be tailored through chemical synthesis. Thus, from the perspective of device fabrication to consider, polymer-based devices (ITO/PAzo-OCH₃/Al and ITO/PAzo-Br/Al) are more suitable as nonvolatile devices.

For considering the effect of the film thickness on the device performance, we studied the data storage performance of the ITO/polymer (70 nm)/Al devices (Fig. S5, Supplementary Material). The results suggested that ITO/PAzo-OCH₃ (70 nm)/Al, ITO/PAzo-Br (70 nm)/Al exhibited turn-on threshold voltages of about –2.3, –3.5 V respectively. Compared to ITO/polymer (100 nm)/Al, the turn-on threshold voltages of ITO/polymer (70 nm)/Al slightly decreased (Fig. S6, Supplementary Material). Thus, the memory effect was almost kept unchanged when the thickness of film was decreased from 100 nm to 70 nm.

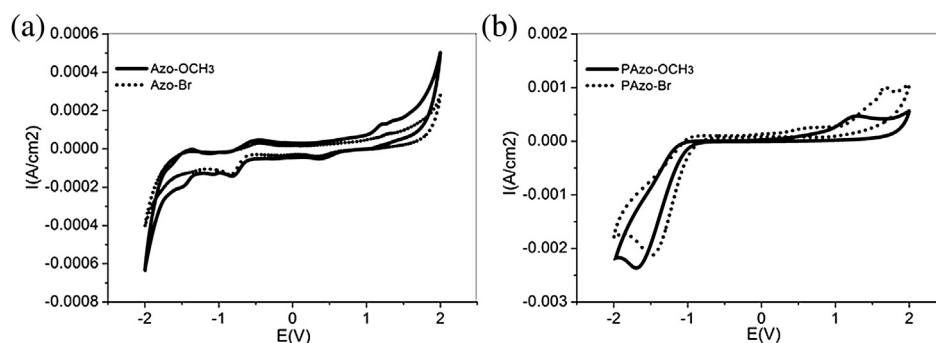


Fig. 2. (a) Cyclic voltammetry (CV) curves of Azo-OCH₃ and Azo-Br in DMF solution (10^{-3} mol/L) with 0.1 M *n*-Bu₄NPF₆ as the supporting electrolyte; (b) cyclic voltammetry (CV) curves of PAzo-OCH₃ and PAzo-Br film on ITO substrate in acetonitrile solution with 0.1 M *n*-Bu₄NPF₆ as the supporting electrolyte.

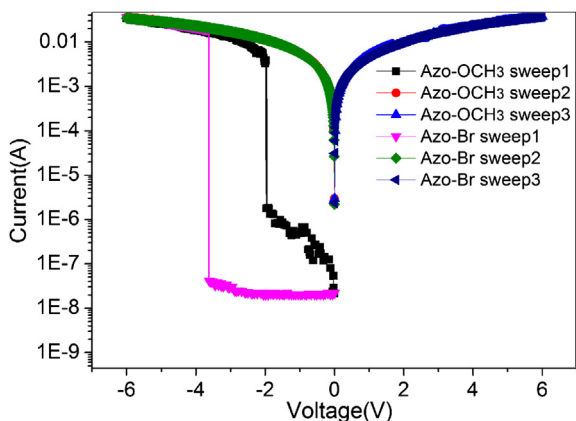


Fig. 3. Current–voltage (I – V) characteristics of the azo organic molecule memory devices.

The stabilities of all these devices under a constant stress of -1 V are shown in Figs. 5 and 6. Under a constant stress of -1 V, no obvious degradation in current is observed for both ON and OFF states for at least 100 min during the readout test. These devices are stable for at least 10^8 continuous read pulses of -1 V, as shown in the inset of Figs. 5 and 6. These results indicate that these polymer memory devices all exhibit good stability.

3.6. Morphology of films

The thin film surface image and roughness were examined by atomic force microscopy at room temperature in a tapping mode, as shown in Fig. 7. The film surface height images of Azo-OCH₃, Azo-Br, PAzo-OCH₃ and PAzo-Br were examined by using atomic force microscopy (AFM) after 12 h of thermal annealing at 110 °C, the scan size of the images is $1 \times 1 \mu\text{m}^2$.

The surface morphology of the vacuum evaporated thin films of Azo-OCH₃ and Azo-Br according to AFM scanning showed surface with root-mean-square roughness of 1.01 and 0.79 nm, respectively; the surface morphology of the spin-coated thin films of PAzo-OCH₃ and PAzo-Br according to AFM scanning showed surface with root-mean-square roughness of 0.35 and 0.30 nm, respectively. The results suggest that the azo polymer films could provide smoother surface than the azo organic molecule films

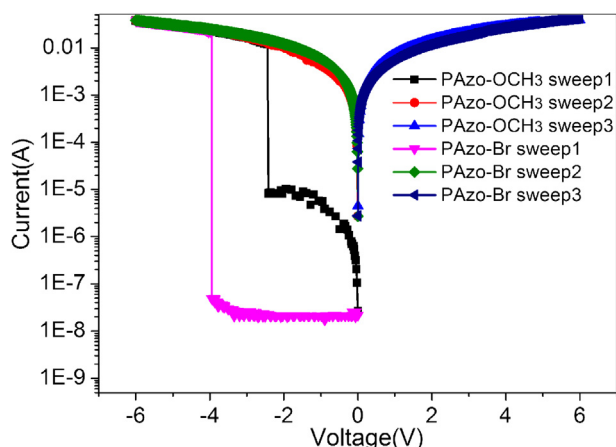


Fig. 4. Current–voltage (I – V) characteristics of the azo polymer memory devices.

[33,34]. The small surface roughness in the AFM images of the polymer films suggests the good quality films [32,35]. Compared to the vacuum evaporated thin films of Azo-OCH₃ and Azo-Br, the spin-coated thin films of PAzo-OCH₃ and PAzo-Br are more favorable in fabricating as memory devices.

3.7. Proposed storage mechanism

The HOMO, LUMO and molecular ESP surfaces of Azo-OCH₃, Azo-Br, PAzo-OCH₃ and PAzo-Br are shown in Table 2. The HOMO surface represents the localization of electron density on the electron donor in the ground state and the LUMO surface represents the localization of electron density on the electron acceptor in the excited state [36]. Through analysis of the electron density change from the HOMO to LUMO surfaces, we can judge how the charge-separated state will exist after the electric field is applied [37]. The results of theoretical calculation indicate that the HOMO of Azo-OCH₃ and PAzo-OCH₃ is located on the ethylamino and methoxyphenyl electron donor moieties, whereas the LUMO of them is located on the azobenzene, cyano electron acceptor moieties; the HOMO of Azo-Br and PAzo-Br is located on the ethylamino electron donor moieties, whereas the LUMO of Azo-Br and PAzo-Br is located on the azobenzene, cyano and bromophenyl electron acceptor moieties. When electron density concentrated on the HOMO orbital, the memory devices are in the OFF state. Under excitations with sufficient energy, electrons in the ground state can transit to the various excited states and a charge-transfer (CT) interaction can occur between the electron donor moieties and the electron acceptor moieties. At this stage, the majority of the charge traps (azobenzene and cyano electron acceptor moieties) are filled, and a “trap-free” environment with higher charge-carrier mobility is formed [38], then a stable CT state is formed. The memory devices are therefore transited from the OFF state to the ON state. This indicates that the electron transfer subsequent to the excitation of the electron donor moieties leads to the intra or intermolecular CT state [24,38–40]. The theoretical high dipole moment of Azo-OCH₃ (9.04 D), Azo-Br (11.33 D), PAzo-OCH₃ (8.24 D) and PAzo-Br (12.11 D) probably leads to a more stable CT complex [37,38,41]. Meanwhile, from the ESP surfaces of Azo-OCH₃, Azo-Br, PAzo-OCH₃ and PAzo-Br, it can be seen that there are some negative regions. These negative regions can serve as “traps”. However, the traps in them are deep and the filled traps cannot be detrapped easily due to the strong electron-withdrawing abilities of the azobenzene and cyano electron acceptor moieties. Thus, once a high-conductivity state is formed, the memory devices will not return to the low-conductivity state [42]. Thus the ITO/organic molecule/Al devices and the ITO/polymer/Al devices all exhibit WORM type memory.

The results were similar with the reported devices of PVK-AZO-NO₂ and PVK-AZO-2CN [24,38], in which electron-withdrawing groups lead to a stable charge-transfer (CT) complex and result in a nonvolatile memory performance. Compared to PVK-AZO-NO₂ and PVK-AZO-2CN, we introduced the different terminal group methoxyphenyl electron donor and bromophenyl electron acceptor to the end of azo organic molecules and azo polymers respectively. Since the contribution of the terminal electron groups with the charge-transfer (CT) process is opposite, Azo-OCH₃ and Azo-Br exhibit different memory performance in some aspects, such as switching voltage and ON/OFF ratio. PAzo-OCH₃ and PAzo-Br also preserve the differences.

3.8. Charge transport mechanism

Further information about the charge transport mechanism of ITO/Azo-OCH₃/Al device, ITO/Azo-Br/Al device, ITO/PAzo-OCH₃/Al device and ITO/PAzo-Br/Al device can be obtained from the I – V

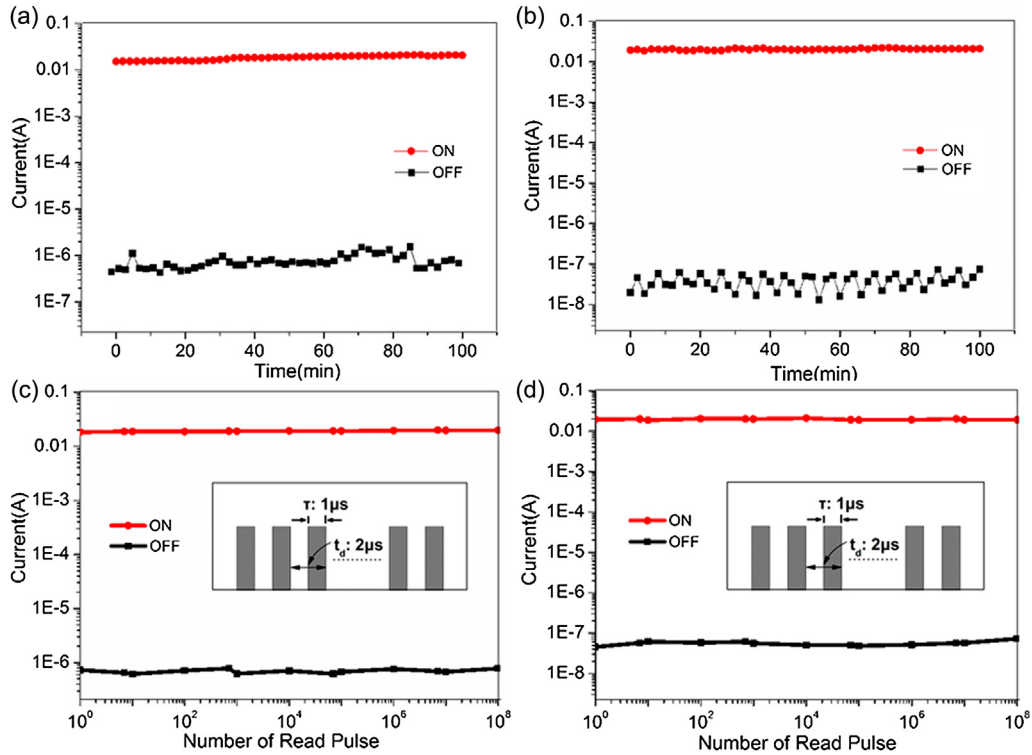


Fig. 5. Retention times on the ON and OFF states of (a) ITO/Azo-OCH₃/Al device and (b) ITO/Azo-Br/Al device under a constant stress of -1 V; effect of read pulse of -1 V on the ON and OFF states of (c) ITO/Azo-OCH₃/Al device and (d) ITO/Azo-Br/Al device.

curves in OFF and ON states according to various theoretical models. Figs. 8a and 9a show that the I - V characteristics for ITO/Azo-OCH₃/Al device and ITO/PAzo-OCH₃/Al device of the low conductivity state can be fitted with the form $J \propto 9\epsilon_i\mu V^2/8d^3$,

where μ is the mobility of charge carriers and ϵ_i is the dynamic permittivity of the insulator and d is the thickness of film. Thus the low conductivity state of ITO/Azo-OCH₃/Al device and ITO/PAzo-OCH₃/Al device can be fitted with the space charge limited

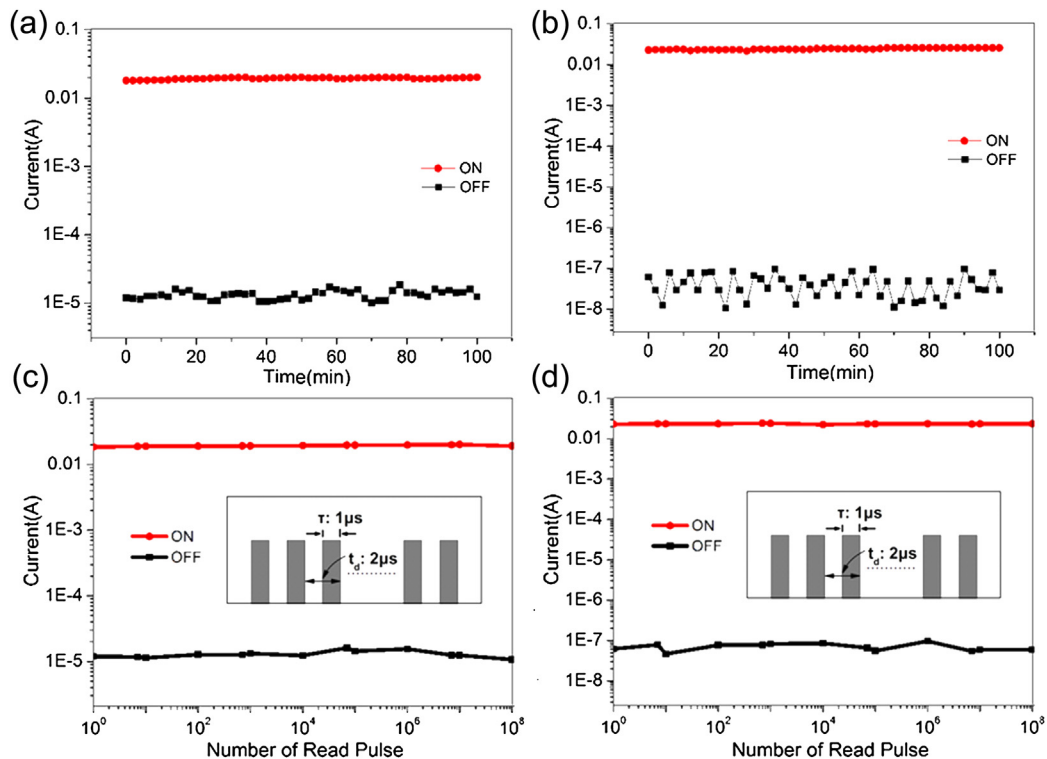


Fig. 6. Retention times on the ON and OFF states of (a) ITO/PAzo-OCH₃/Al device and (b) ITO/PAzo-Br/Al device under a constant stress of -1 V; effect of read pulse of -1 V on the ON and OFF states of (c) ITO/PAzo-OCH₃/Al device and (d) ITO/PAzo-Br/Al device.

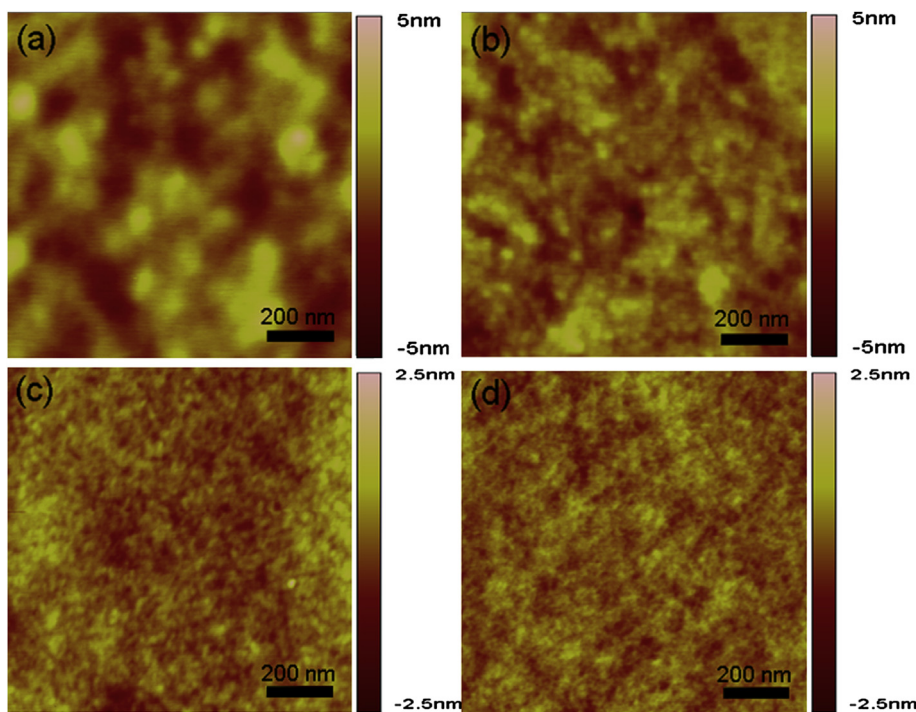
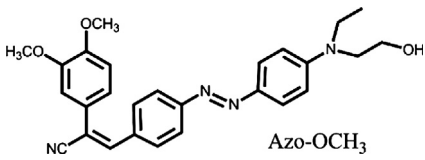
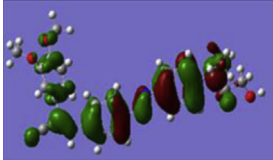
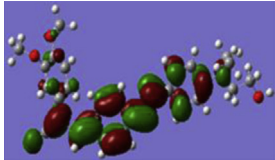
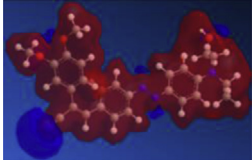
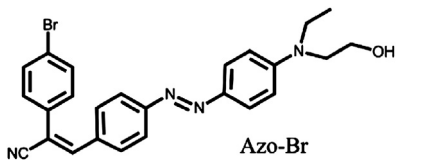
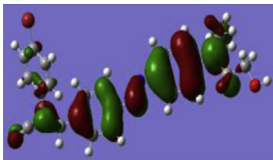
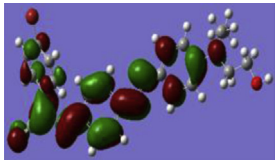
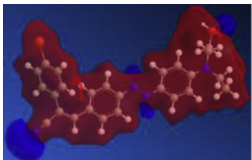
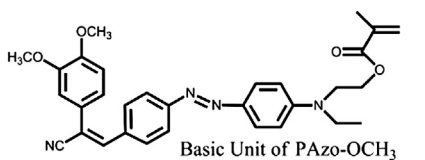
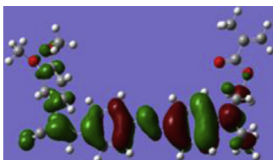
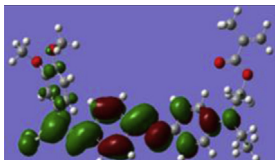
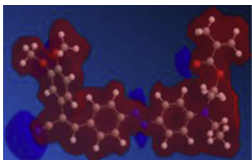
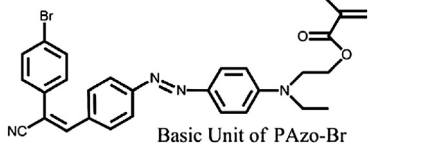
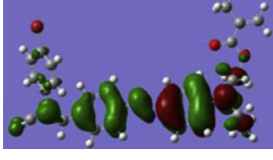
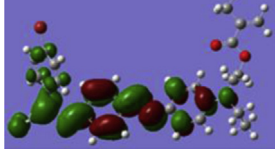
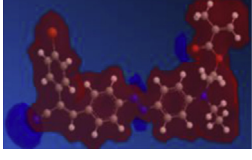


Fig. 7. AFM height images of (a) Azo-OCH₃ (b) Azo-Br (c) PAzo-OCH₃ (d) PAzo-Br, the scan size of the images is 1 × 1 μm².

Table 2

HOMO, LUMO and ESP surfaces of Azo-OCH₃, Azo-Br, PAzo-OCH₃ and PAzo-Br.

Molecular structure	HOMO	LUMO	ESP
 Azo-OCH ₃			
 Azo-Br			
 Basic Unit of PAzo-OCH ₃			
 Basic Unit of PAzo-Br			

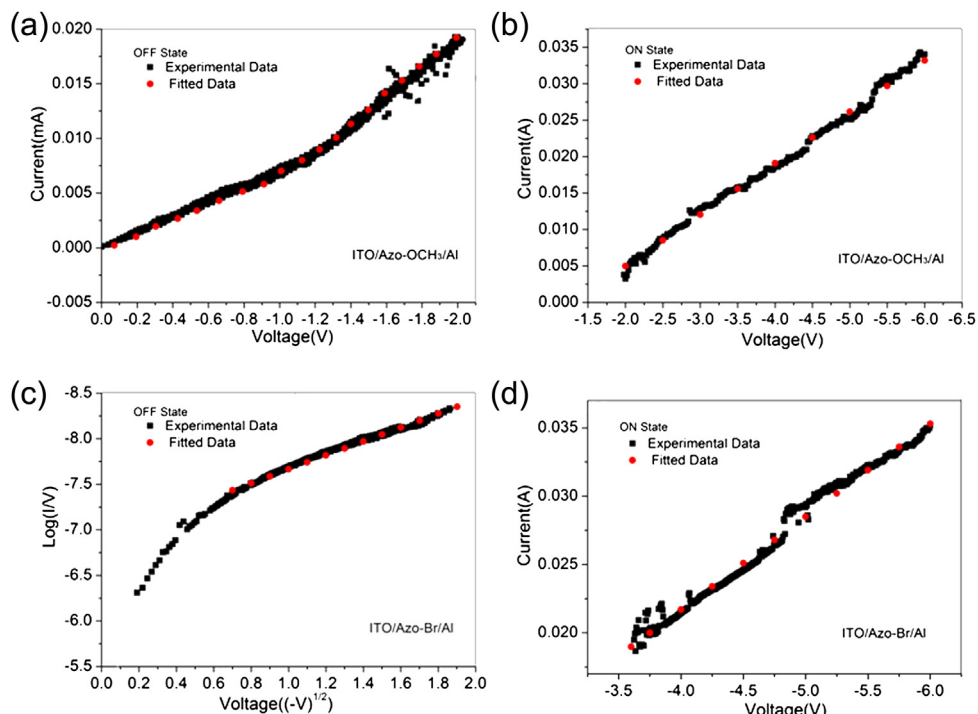


Fig. 8. Experimental and fitted data of I - V curves for ITO/Azo-OCH₃/Al device and ITO/Azo-Br/Al device in the OFF and ON states. Panels a and b are the OFF state with the SCLC model and the ON state with the ohmic current model for ITO/Azo-OCH₃/Al device. Panels c and d are the OFF state with the Poole Frenkel model (-0.49 to -3.6 V) and the ON state with the ohmic current model for ITO/Azo-Br/Al device.

current (SCLC) model [43]. Figs. 8c and 9c show that the low conductivity state of ITO/Azo-Br/Al device and ITO/PAzo-Br/Al device can be elucidated as Poole-Frenkel (PF) emission in terms of the plots of $\log(I/V)$ versus $V^{1/2}$ found to be linear [44]. The PF emission is probably attributed to charge transport of

organic and polymeric materials filled with charge traps [34]. The electron-accepting terminal moieties bromophenyl probably facilitate the process of the carrier captured and released due to the stronger electron withdraw ability of Azo-Br and PAzo-Br [34,45]. Thus the low conductivity state of ITO/Azo-Br/Al device

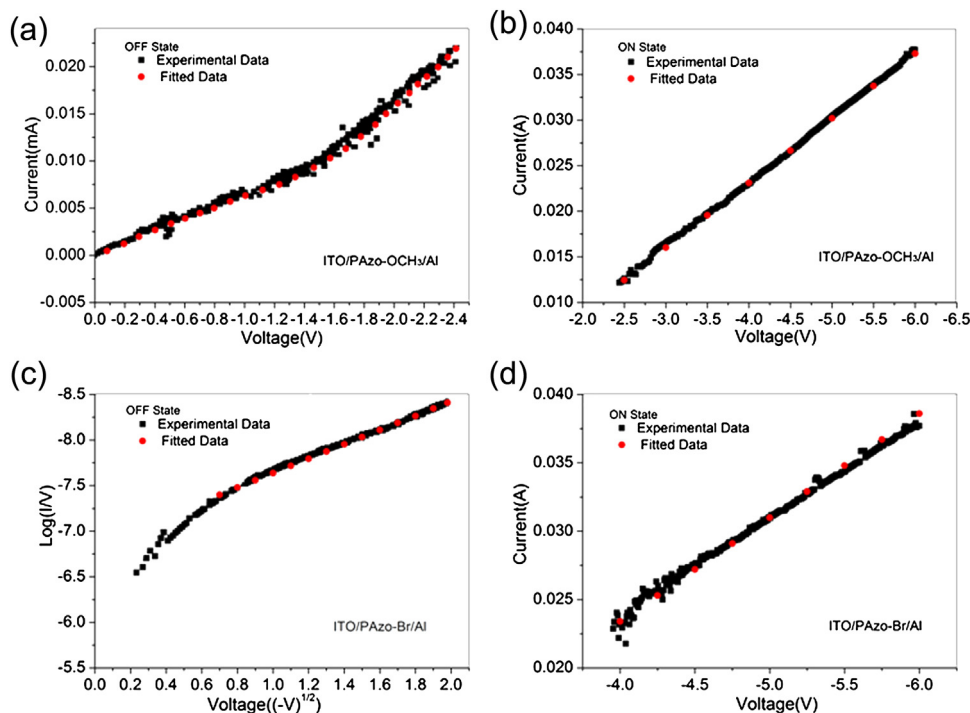


Fig. 9. Experimental and fitted data of I - V curves for ITO/PAzo-OCH₃/Al device and ITO/PAzo-Br/Al device in the OFF and ON states. Panels a and b are the OFF state with the SCLC model and the ON state with the ohmic current model for ITO/PAzo-OCH₃/Al device. Panels c and d are the OFF state with the Poole Frenkel model (-0.49 to -4 V) and the ON state with the ohmic current model for ITO/PAzo-Br/Al device.

and ITO/PAzo-Br/Al device can be fitted with Poole–Frenkel (PF) emission. Figs. 8b and d and Fig. 9b and d show that the I – V characteristics for all memory devices of the high conductivity state are linear and can be fitted with the ohmic model. This indicates that in the ON state the charge transport is dominated by the ohmic model [45,46].

4. Conclusions

In this paper, we have successfully synthesized two new azo organic molecules Azo-OCH₃ and Azo-Br with different terminal electron moieties and their homopolymers for nonvolatile electronic memory materials. The ITO/organic molecule/Al devices and the ITO/polymer/Al devices all exhibit WORM memory behavior. Both the ON and OFF states of the devices investigated are stable under a constant read voltage stress of -1 V and even can endure 10^8 read cycles under a pulse read voltage. The OFF state of ITO/Azo-OCH₃/Al device and ITO/PAzo-OCH₃/Al device can be fitted with the space charge limited current (SCLC) model while the OFF state of ITO/Azo-Br/Al device and ITO/PAzo-Br/Al device can be fitted with Poole–Frenkel (PF) emission. The ON state of all memory devices can be fitted with the ohmic model. Azo-OCH₃, Azo-Br, PAzo-OCH₃ and PAzo-Br are all p-type materials. Both Azo-OCH₃ and PAzo-OCH₃ based devices have an advantage of possessing low turn-on threshold voltage due to the lower hole-injection barrier, which means low-power consumption. Polymers have successfully retained the storage performance of organic molecules. Moreover, polymer-based memory devices fabricated by spin coating polymer materials have the advantages of easy fabrication, high mechanical flexibility, good stability and many other advantages. Thus, from the perspective of device fabrication to consider, we have successfully achieved the advantages of easy fabrication, low-cost and low-power consumption without destroying the storage performance.

Acknowledgments

The authors graciously thank the Chinese Natural Science Foundation (21071105 and 21176164), Chinese–Singapore Joint Project (2012DFG41900), the Specialized Research Fund for the Doctoral Program of Higher Education of China (grant no. 20113201130003), and the project funded by the Priority Academic Program Development (PAPD) of Jiangsu Higher Education Institution.

Appendix A. Supplementary data

Supplementary data related to this article can be found at <http://dx.doi.org/10.1016/j.polymer.2013.04.043>.

References

- [1] Chen Q, Zhao L, Li C, Shi G. *J Phys Chem C* 2007;111:18392.
- [2] Joo WJ, Choi TL, Lee J, Lee SK, Jung MS, Kim N, et al. *J Phys Chem B* 2006;110:23812.
- [3] Kim TW, Choi H, Oh SH, Wang G, Kim DY, Hwang H, et al. *Adv Mater* 2009;21:2497.
- [4] Choi TL, Lee KH, Joo WJ, Lee S, Lee TW, Chae MY. *J Am Chem Soc* 2007;129:9842.
- [5] Kim M, Choi S, Ree M, Kim O. *IEEE Electron Device Lett* 2007;28:967.
- [6] Cho B, Kim TW, Choe M, Wang G, Song S, Lee T. *Org Electron* 2009;10:473.
- [7] Kim TW, Oh SH, Lee J, Choi H, Wang G, Park J, et al. *Org Electron* 2010;11:109.
- [8] Fang J, You H, Chen J, Lin J, Ma D. *Inorg Chem* 2006;45:3701.
- [9] Ling QD, Wang W, Song Y, Zhu CX, Chan DSH, Kang ET, et al. *J Phys Chem B* 2006;110:23995.
- [10] Kim K, Park S, Hahm SG, Lee TJ, Kim DM, Kim JC, et al. *J Phys Chem B* 2009;113:9143.
- [11] Ling QD, Lim SL, Song Y, Zhu CX, Chan DSH, Kang ET, et al. *Langmuir* 2007;23:312.
- [12] Li L, Ling QD, Lim SL, Tan YP, Zhu C, Chan DSH, et al. *Org Electron* 2007;8:401.
- [13] Cho B, Kim TW, Song S, Ji Y, Jo M, Hwang H, et al. *Adv Mater* 2010;22:1228.
- [14] Lee TJ, Chang CW, Hahm SG, Kim K, Park S, Kim DM, et al. *Nanotechnology* 2009;20:135204.
- [15] Li F, Son DI, Seo SM, Cha HM, Kim HJ, Kim BJ, et al. *Appl Phys Lett* 2007;91:122111.
- [16] Lee J, Lee E, Kim S, Bang GS, Shultz DA, Schmidt RD, et al. *Angew Chem Int Ed* 2011;50:4414.
- [17] Liu Y, Lv S, Li L, Shang S. *Synth Metals* 2012;162:1059.
- [18] Wei Y, Gao D, Li L, Shang S. *Polymer* 2011;52:1385.
- [19] Kim TW, Oh SH, Choi H, Wang G, Hwang H, Kim DY, et al. *IEEE Electron Device Lett* 2008;29:852.
- [20] Wang P, Liu SJ, Lin ZH, Dong XC, Zhao Q, Lin WP, et al. *J Mater Chem* 2012;22:9576.
- [21] Ling QD, Song Y, Ding SJ, Zhu C, Chan DSH, Kwong DL, et al. *Adv Mater* 2005;17:455.
- [22] Baek S, Lee D, Kim J, Hong SH, Kim O, Ree M. *Adv Funct Mater* 2007;17:2637.
- [23] Zhang Q, Pan J, Yi X, Li L, Shang S. *Org Electron* 2012;13:1289.
- [24] Liu G, Zhang B, Chen Y, Zhu CX, Zeng L, Chan DSH, et al. *J Mater Chem* 2011;21:6027.
- [25] Salaoru I, Paul S. *Thin Solid Films* 2010;519:559.
- [26] Fan N, Liu H, Zhou Q, Zhuang H, Li Y, Li H, et al. *J Mater Chem* 2012;22:19957.
- [27] Kim DM, Park S, Lee TJ, Hahm SG, Kim K, Kim JC, et al. *Langmuir* 2009;25:11713.
- [28] Fang YK, Liu CL, Chen WC. *J Mater Chem* 2011;21:4778.
- [29] Liu CL, Kurosawa T, Yu AD, Higashihara T, Ueda M, Chen WC. *J Phys Chem C* 2011;115:5930.
- [30] Wang KL, Liu YL, Lee JW, Neoh KG, Kang ET. *Macromolecules* 2010;43:7159.
- [31] Liu SJ, Wang P, Zhao Q, Yang HY, Wong J, Sun HB, et al. *Adv Mater* 2012;24:2901.
- [32] You NH, Chueh CC, Liu CL, Ueda M, Chen WC. *Macromolecules* 2009;42:4456.
- [33] Liu CL, Hsu JC, Chen WC, Sugiyama K, Hirao A. *ACS Appl Mater Interfaces* 2009;1:1974.
- [34] Lee WY, Kurosawa T, Lin ST, Higashihara T, Ueda M, Chen WC. *Chem Mater* 2011;23:4487.
- [35] Hahm SG, Lee TJ, Kim DM, Kwon W, Ko YG, Michinobu T, et al. *J Phys Chem C* 2011;115:21954.
- [36] Li H, Wen Y, Li P, Wang R, Li G, Ma Y, et al. *Appl Phys Lett* 2009;94:163309.
- [37] Li H, Li N, Sun R, Gu H, Ge J, Lu J, et al. *J Phys Chem C* 2011;115:8288.
- [38] Zhang B, Liu G, Chen Y, Wang C, Neoh KG, Bai T, et al. *ChemPlusChem* 2012;77:74.
- [39] Kurosawa T, Chueh CC, Liu CL, Higashihara T, Ueda M, Chen WC. *Macromolecules* 2010;43:1236.
- [40] Liu YL, Ling QD, Kang ET, Neoh KG, Liaw DJ, Wang KL, et al. *J Appl Phys* 2009;105:044501.
- [41] Liu YL, Wang KL, Huang GS, Zhu CX, Tok ES, Neoh KG, et al. *Chem Mater* 2009;21:3391.
- [42] Wang KL, Liu YL, Shih IH, Neoh KG, Kang ET. *Polym Chem* 2010;48:5790.
- [43] Ling QD, Song Y, Lim SL, Teo EYH, Tan YP, Zhu C, et al. *Angew Chem Int Ed* 2006;45:2947.
- [44] Li H, Li N, Gu H, Xu Q, Yan F, Lu J, et al. *J Phys Chem C* 2010;114:6117.
- [45] Li Y, Xu H, Tao X, Qian K, Fu S, Shen Y, et al. *J Mater Chem* 2011;21:1810.
- [46] Liu J, Yin Z, Cao X, Zhao F, Lin A, Xie L, et al. *ACS Nano* 2010;4:3987.